scientific reports

Check for updates

OPEN

Inhibition of breast cancer resistance protein by flavonols: in vitro, in vivo, and in silico implications of the interactions

Kyeong-Ryoon Lee[1,2,5], Min-Ji Kang[3,5], Min Ju Kim[1], Yiseul Im[1,2], Hyeon-Cheol Jeong[1] & Yoon-Jee Chae[3,4]✉

Breast cancer resistance protein (BCRP), a member of the ATP-binding cassette transporter family, plays a key role in the efflux of various drugs and is linked to multidrug resistance in cancer therapy. Flavonoids, particularly those with a flavonol backbone, have shown promise as inhibitors of BCRP activity; however, their specific inhibitory effects are not fully understood. This study explored the inhibitory effects of 77 flavonols on BCRP and identified 22 compounds with significant inhibitory activity. Among them, 14 flavonols had half-maximal inhibitory concentrations (IC_{50}) values below 5 μM, effectively reversing BCRP-mediated resistance to SN-38 in vitro. Molecular docking analysis revealed key interactions between flavonols and BCRP, including π-stacking, hydrogen bonding, and hydrophobic interactions. Structural modifications, including hydroxylation and methylation, enhanced the binding affinity of the flavonols. In vivo studies with 3,4′-dimethoxyflavone and 3,6,3′,4′-tetramethoxyflavone resulted in increased systemic exposure to sulfasalazine, a known BCRP substrate. These findings provide mechanistic insights into flavonol-BCRP interactions, suggesting their potential to enhance drug exposure and efficacy. Future research should focus on clinical applications to explore the therapeutic potential of these flavonols for improved drug responses.

Keywords Breast cancer resistance protein, Flavonols, Drug interactions, Drug resistance, SN-38

Breast cancer resistance protein (BCRP), encoded by the *ABCG2* gene, is a member of the adenosine triphosphate (ATP)-binding cassette transporter superfamily. With a molecular weight of 72 kDa, BCRP functions as an efflux transporter, actively pumping various compounds out of cells[1]. Structurally, BCRP is composed of a single polypeptide chain that contains six transmembrane helices and a cytoplasmic nucleotide-binding domain. BCRP recognizes a wide range of substrates, including clinically important and structurally diverse drugs such as rosuvastatin, topotecan, irinotecan, sulfasalazine, and chlorothiazide, as well as endogenous molecules like bile acids and estrogens[2–6]. It is expressed in multiple tissues, where its localization and function significantly influence drug pharmacokinetics. For instance, on the apical side of intestinal cells, BCRP reduces drug absorption, whereas its expression on the canalicular membrane of hepatocytes and the proximal tubules of renal cells promotes drug excretion into bile or urine, respectively. Furthermore, BCRP in barrier tissues such as the brain, testis, and placenta limits drug penetration into these tissues, thereby impacting drug distribution[7–9]. Therefore, BCRP plays a critical role in regulating drug concentrations in the body, ultimately affecting therapeutic efficacy and toxicity risk.

Clinically important roles of BCRP have been demonstrated through pharmacogenetic and drug interaction studies[10,11]. For example, individuals with the 421CA or 421AA genotypes, which encode BCRP having a reduced-function, exhibit a 1.9-fold increase in the maximum plasma concentration of rosuvastatin compared with those with the 421CC wild-type homozygous genotype[12]. Additionally, the half-life of oxypurinol, the active metabolite of allopurinol and a BCRP substrate, is prolonged by 1.8-fold in individuals homozygous for the p.Q141K variant, which is encoded by 421 C > A, owing to reduced excretion[13]. Similarly, BCRP-mediated

[1]Laboratory Animal Resource Center, Korea Research Institute of Bioscience and Biotechnology, Cheongju 28116, Republic of Korea. [2]Department of Bioengineering, University of Science and Technology, Daejeon 34113, Republic of Korea. [3]College of Pharmacy, Woosuk University, Wanju 55338, Republic of Korea. [4]Research Institute of Pharmaceutical Sciences, Woosuk University, Wanju 55338, Republic of Korea. [5]These authors contributed equally to this work: Kyeong-Ryoon Lee and Min-Ji Kang. ✉email: yjchae@woosuk.ac.kr

drug transport can be inhibited by various concomitant drugs such as gefitinib, imatinib, bosutinib, and cyclosporine, leading to clinically significant drug interactions. Fostamatinib, a BCRP inhibitor, increases the plasma concentration of rosuvastatin, a BCRP substrate, by approximately two-fold[14]. While such interactions raise concerns about the potential side effects from increased drug exposure, they also present opportunities to enhance the bioavailability of drugs with low absorption due to BCRP activity. Given its pivotal role in influencing the pharmacokinetics, efficacy, and toxicity, understanding the interplay between BCRP and concomitant substances is crucial for optimizing therapeutic strategies and minimizing adverse drug interactions.

BCRP is also implicated in cancer drug resistance, further emphasizing its clinical importance[15]. Since its isolation from the drug-resistant breast cancer cell line MCF-7/AdrVp, BCRP expression has been observed in various cancer cells. Genetic polymorphisms in BCRP are associated with cancer prognosis and survival. The 421CC genotype (wild type) significantly correlates with poor survival outcomes in patients with diffuse large B-cell lymphoma[16]. Similarly, a meta-analysis suggests that the 421CA polymorphism may play a protective role against cancer by reducing overall cancer risk[17].

Flavonoids are a diverse class of polyphenolic secondary metabolites predominantly found in plants, representing a significant component of the human diet. These compounds are categorized into subgroups such as flavonols, anthocyanins, and flavanones based on their structural characteristics[18]. Increasing recognition of their diverse physiological activities has led to the development of several dietary supplements and clinical trials for disease treatment. One of the most studied flavonoids is quercetin, found in berries, green tea, and grains. The chemopreventive effects of quercetin, particularly in colorectal cancer, have been extensively investigated. The mechanisms underlying its efficacy include cell cycle arrest, enhanced apoptosis, antioxidant activity, modulation of estrogen receptors, regulation of signaling pathways, and inhibition of metastasis and angiogenesis[19]. Similarly, preclinical studies have demonstrated the cardioprotective effects of morin. In a myocardial necrosis model, oral administration of morin to rats improved antioxidant capacity and reduced apoptosis, with its cardioprotective mechanism attributed to modulation of the MAPK/NF-κB/TNF-α pathway[20]. Flavonoids also interact with pharmacologically significant membrane transporters, such as BCRP, multidrug resistance 1 (MDR1), and organic cation transporter 2 (OCT2)[21,22]. Especially, specific flavonoids, including quercetin, kaempferol, apigenin, and naringenin, have been shown to inhibit BCRP activity[23]. However, the potential BCRP-inhibitory effects of many flavonoids remain unexplored. Considering the clinically significant roles of BCRP and the widespread use of flavonoids, this knowledge gap highlights the need for further research to assess the potential risks associated with flavonoid co-administration with BCRP substrate drugs.

To foster a broader understanding of the relationship between flavonoids and BCRP, this study aimed to evaluate the BCRP inhibitory potential of flavonoids, with a particular focus on the flavonol structure. In addition to assessing these inhibitory effects, we investigated potential in vivo pharmacokinetic interactions involving flavonols. Furthermore, we explored their ability to overcome multidrug resistance, a major challenge in clinical treatment, particularly in cancer therapy. Based on these findings, we propose potential therapeutic and pharmacological applications of flavonols with high BCRP-inhibitory activity, offering novel opportunities to enhance drug bioavailability, improve treatment efficacy, and address resistance mechanisms in multidrug-resistant conditions.

Materials and methods

Materials

The 3-(4,5-dimethylthiazol-2-yl)−2,5-diphenyltetrazolium bromide (MTT) used in this study was obtained from Alfa Aesar (Haverhill, MA, USA). Fetal bovine serum (FBS), Hanks' balanced salt solution (HBSS), and 4-(2-hydroxyethyl)−1-piperazineethanesulfonic acid (HEPES) were obtained from Gibco (Grand Island, NY, USA). Prazosin, SN-38, Dulbecco's Modified Eagle's medium (DMEM) with high glucose, nonessential amino acids (NEAA), trypsin-ethylenediaminetetraacetic acid (EDTA), penicillin/streptomycin solution, phosphate-buffered saline (PBS), poly-D-lysine, Triton X-100, novobiocin, formic acid, and dimethyl sulfoxide (DMSO) were sourced from Sigma-Aldrich (St. Louis, MO, USA). High-performance liquid chromatography (HPLC)-grade methanol, acetonitrile, and water were purchased from J. T. Baker (Phillipsburg, NJ, USA). All other chemicals were of analytical grade.

Structural information of flavonol derivatives

A total of 77 flavonoids were supplied by the Korea Chemical Bank of the Korea Research Institute of Chemical Technology (Daejeon, Korea) (Supplementary Table 1). Each compound shared a common flavonol backbone structure (Fig. 1A) and featured various functional groups, including methyl, hydroxy, 3-methyl-2-buten, propionic acid, methoxy, and glycosides.

Cell maintenance

Madin-Darby canine kidney II (MDCKII) cells stably expressing human BCRP and MDCKII-mock cells were used to evaluate the interactions between flavonols and BCRP transporters. MDCKII-BCRP cells were kindly provided from Prof. Sukjae Chung (Seoul National University, Republic of Korea). The stable expression and functionality of BCRP in these cell lines have been validated in previous studies[24–26] ensuring their reliability for this study. Cells were cultured in DMEM with high glucose, supplemented with 10% FBS, 100 U/mL penicillin, 0.1 mg/mL streptomycin, and 5 mM NEAA. All cell incubations, including cell culture and compound treatment, were performed at 37 °C in a humidified CO_2 incubator maintained at 5% CO_2 and 95% relative humidity. Cells were passaged at 70–80% confluence using trypsin-EDTA to maintain optimal growth conditions.

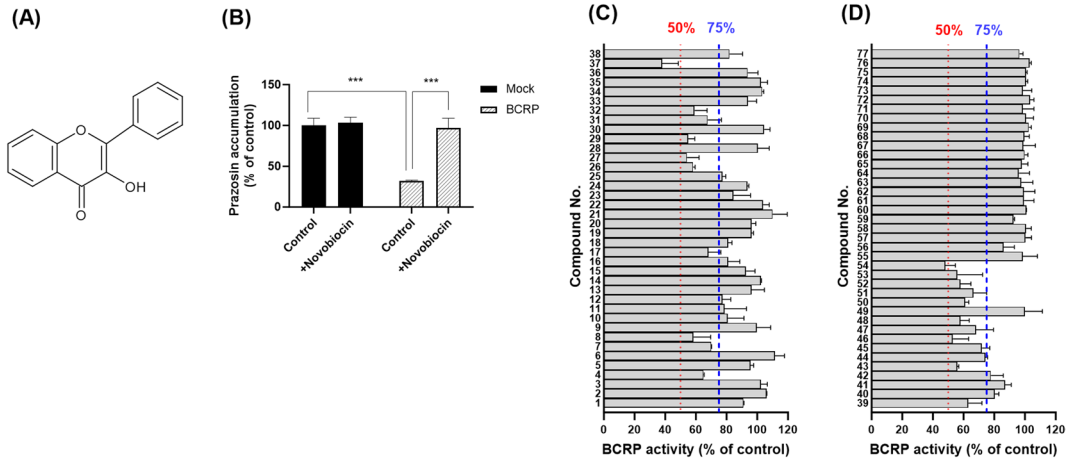

Fig. 1. Flavonol structure and screening assay results. (**A**) Flavonol backbone structure. (**B**) BCRP activity in the absence or presence of the positive inhibitor (novobiocin, 5 μM) in MDCKII-mock and MDCKII-BCRP cells. (**C** and **D**) BCRP activity in the absence or presence of flavonols (2 μM) in MDCKII-BCRP. Cells were incubated for 20 min after the treatment. Blue and red dotted lines represent 75% and 50% of BCRP activity (% of control), respectively. *** denotes $p < 0.001$. Data are expressed as the mean ± SD ($n = 3$).

Functional Inhibition study

The inhibitory potential of flavonols on the BCRP transporter was assessed using an accumulation assay with prazosin as a substrate. MDCKII-BCRP cells were seeded in 96-well plates (SPL Life Science, Korea) at a density of 5×10^4 cells/well and allowed to grow to confluence for 24 h. Before the assay, cells were washed twice with pre-warmed transport buffer (HBSS containing 10 mM HEPES, pH 7.4) and incubated at 37 °C for 30 min to ensure that the cells are equilibrated to a stable condition ready for the uptake assay.

The accumulation assay was initiated by adding 5 μM prazosin in the presence or absence of flavonols to the cells. Initially, the flavonols were screened for BCRP inhibition at a concentration of 2 μM, and compounds that inhibited BCRP activity by more than 25% were selected for half-maximal inhibitory concentration (IC_{50}) determination. For IC_{50} evaluation, selected flavonols were tested at concentrations of 0, 0.01, 0.4, 2, 10, and 30 μM. Novobiocin served as a positive control inhibitor. DMSO concentration did not exceed 1% to prevent cytotoxic effects. Cells were incubated with test compounds prepared in transport buffer for 20 min at 37 °C. After incubation, the cells were quickly washed three times with ice-cold PBS and lysed by shaking at 100 rpm with 0.1% Triton X-100 in PBS for at least 30 min to ensure complete lysis. The lysates were collected and stored at − 80 °C until HPLC analysis.

Reversal of BCRP-mediated drug resistance by flavonols

We evaluated the effects of flavonols on BCRP-mediated drug resistance. We used SN-38, a cytotoxic agent and a known BCRP substrate, at different concentrations (0, 0.005, 0.05, 0.5, 5, 50 μM) with 14 flavonols (5 μM) which strongly inhibited BCRP in vitro. The selection of 5 μM for flavonol treatment was based on our preliminary internal experiments, which confirmed that concentrations up to 5 μM did not induce significant cytotoxicity in either MDCKII-mock or MDCKII-BCRP cells (data not shown). Novobiocin (5 μM) was used as a positive control to validate the reliability of the experiments. After incubation of MDCKII-mock and MDCKII-BCRP cells with SN-38 in the presence or absence of flavonols for 48 h, cell viability was measured using the MTT assay. To quantify the ability of flavonols to reverse BCRP-mediated resistance, we calculated the reverse fold (RF) for each cell line by comparing the half-maximal cytotoxic concentration (CC_{50}) of SN-38 in the absence and presence of flavonols. The RF values for MDCKII-mock and MDCKII-BCRP cells ($RF_{MDCKII\text{-}mock}$ and $RF_{MDCKII\text{-}BCRP}$) were determined and the total reverse fold (RF_t) was calculated by dividing the CC_{50} of SN-38 in MDCKII-BCRP cells by that in MDCKII-mock cells.

Molecular docking

A molecular docking study was conducted to investigate interactions between BCRP and 14 flavonols that strongly inhibited BCRP in vitro ($IC_{50} < 5$ μM). The 3D crystal structure of the BCRP transporter was obtained from the Protein Data Bank (BCRP structure ID: 6ffc) (https://www.rcsb.org). The molecular structures of novobiocin, a representative BCRP inhibitor, and flavonols were retrieved from PubChem (https://pubchem.ncbi.nlm.nih.gov) in SDF format. Docking was conducted using CB-Dock 2 (https://cadd.labshare.cn/cb-dock2)[27] which identified potential binding sites on the BCRP transporter and docked flavonols within these pockets. Binding energies of flavonols were calculated automatically by CB-Dock 2. Following docking, the interaction between the BCRP transporter and flavonols was analyzed using BIOVIA Discovery Studio Visualizer v24.1.0. (Dassault Systemes Biovia Corp., San Diego, CA, USA). Non-covalent interactions were systematically identified, including conventional hydrogen bonds, hydrophobic interactions (such as van der Waals forces and alkyl interactions), π–π stacking, π–sigma interactions, π–cation interactions, and unfavorable donor–donor interactions, with key BCRP amino acid residues.

In vivo interactions of flavonols with BCRP

To further investigate the in vivo effects of potent BCRP inhibitors, we conducted a pharmacokinetic interaction study using sulfasalazine, a well-known BCRP substrate, in Sprague-Dawley (SD) rats. Male SD rats (8 weeks old; 250–270 g) were obtained from Koatech Inc. (Pyeongtaek, Gyeonggi, Republic of Korea) and acclimatized for 1 week before the experiment. The rats were housed under standard laboratory conditions with a 12-h light/dark cycle, controlled temperature (22 ± 2 °C), and relative humidity (50–60%). All procedures complied with institutional guidelines for the care and use of laboratory animals, and ethical approval was obtained from the Institutional Animal Care and Use Committee (IACUC) of the Korea Research Institute of Bioscience and Biotechnology (approval number, KRIBB-AEC-24009). Before drug administration, animals were fasted overnight with free access to water. Rats were randomly assigned to three groups ($n = 5$ per group): one receiving oral administration of sulfasalazine (2 mg/kg) alone, one receiving sulfasalazine (2 mg/kg) co-administered with 3,4′-dimethoxyflavone (5 mg/kg), and one receiving sulfasalazine (2 mg/kg) co-administered with 3,6,3′,4′-tetramethoxyflavone (5 mg/kg). The dosing solution was prepared in N, N-dimethylacetamide (DMAC), Cremorphor EL, 20% of 2-hydroxypropyl-ß-cyclodextrin (HPβCD) in water (1:1:8). Blood samples were collected via the jugular vein at designated time points (0, 0.25, 0.5, 1, 2, 4, 6, 8, and 24 h post dose) by serial sampling from the same animals. Plasma was then separated by centrifugation at 13,000 rpm for 10 min at 4 °C and stored at − 80 °C until analysis.

HPLC-FLD and LC-MS/MS analysis

The intracellular concentration of prazosin was quantified using a Shimadzu LC-20 HPLC system (Shimadzu Co., Kyoto, Japan) equipped with a fluorescence detector (FLD; RF-20 A, Shimadzu Co.). A reverse-phase HPLC column (Hypersil Gold C18 column, 50 mm × 4.6 mm id, 5 µm; Thermo Scientific, NY, USA) was used, with quinidine as the internal standard (IS). The mobile phase comprised 40% ammonium formate (50 mM) in water and 60% methanol, delivered at a flow rate of 1 mL/min. Cell lysate samples (20 µL) were mixed with 180 µL of methanol containing the IS (100 ng/mL), followed by centrifugation at 12,000 rpm for 4 min to precipitate proteins. The resulting supernatants were then transferred to HPLC vials for analysis. Prazosin was detected at excitation/emission wavelengths of 335/415 nm, and data were analyzed using LC Solution Software (Version 1.25; Shimadzu Co.). The amount of prazosin accumulated in the cells was normalized to protein concentrations determined via the bicinchoninic acid (BCA) protein assay.

Plasma levels of sulfasalazine, 3,4′-dimethoxyflavone, and 3,6,3′,4′-tetramethoxyflavone in rats were measured using a liquid chromatography-tandem mass spectrometry (LC-MS/MS) system. This system comprised an Agilent 1200 HPLC system linked to an API 4000 triple-quadrupole mass spectrometer. The mass spectrometer was operated in positive electrospray ionization (ESI+) mode with multiple reaction monitoring (MRM). The m/z transitions were monitored at 399.06 → 380.80 for sulfasalazine, 283.11 → 268.20 for 3,4′-dimethoxyflavone, 343.04 → 328.00 for 3,6,3′,4′-tetramethoxyflavone, and 237.00 → 194.00 for carbamazepine (IS). For sample preparation, 20 µL of plasma was mixed with 100 µL of methanol containing IS (50 ng/mL), followed by centrifugation at 13,000 rpm for 4 min at 4 °C. Chromatographic separation was performed using a reversed-phase Xterra MS C18 column (2.1 × 50 mm, 3.5 µm; Waters, Milford, MA, USA) with gradient elution. The mobile phase consisted of 5 mM ammonium formate in water and 0.1% formic acid in acetonitrile at a flow rate of 0.35 mL/min.

Data analysis

IC_{50} values of the flavonols for BCRP activity were calculated using GraphPad 10.0.3 (GraphPad Software Inc., San Diego, CA, USA) with the following equation:

$$BCRP\ activity\ (\%\ of\ control) = \frac{100}{1 + \left(\frac{C}{IC_{50}}\right)^{n}}$$

where C represents the inhibitor concentration, and n denotes the Hill coefficient, which was estimated by nonlinear regression analysis using the variable slope (four-parameter logistic) model. BCRP activity was calculated using the following equation:

$$BCRP\ activity\ (\%\ of\ control) = \frac{(Prazosin\ in\ MDCKII_{mock,\ inhibitor}) - (Prazosin\ in\ MDCKII_{BCRP,\ inhibitor})}{(Prazosin\ in\ MDCKII_{mock,\ no\ inhibitor}) - (Prazosin\ in\ MDCKII_{BCRP,\ no\ inhibitor})} \times 100$$

The CC_{50} values of SN-38 in the presence or absence of flavonols were calculated using the following equation:

$$Cell\ viability\ (\%\ \text{of control}) = \frac{100}{1 + \left(\frac{C}{CC_{50}}\right)^{n}}$$

where C represents the SN-38 concentration, and n denotes the Hill coefficient.

Pharmacokinetic parameters were determined using WinNonlin software (Certara USA Inc., Princeton, NJ, USA). The following parameters were calculated using noncompartmental analysis: area under the plasma concentration–time curve from time zero to the last quantifiable point (AUC_{last}), area under the plasma concentration–time curve from time 0 to infinity (AUC_{inf}), maximum concentration (C_{max}), time to reach maximum concentration (T_{max}), and elimination half-life ($t_{1/2}$). The AUC_{last} and AUC_{inf} were determined using the trapezoidal rule and extrapolation to infinity. C_{max} and T_{max} were obtained directly from the plasma concentration–time data, while $t_{1/2}$ was calculated based on the terminal slope of the plasma concentration–time profile.

Statistical analyses were performed using the Student's t-test for comparisons between two groups. *p*-value < 0.05 was considered statistically significant. Data were presented as mean ± standard deviation (SD).

Results

Screening for inhibitory potential of flavonols on BCRP

To assess the inhibitory potential of 77 flavonols on BCRP activity, MDCKII-mock and MDCKII-BCRP cells were treated with prazosin (5 μM) in the presence of flavonols at a concentration of 2 μM. In MDCKII-BCRP cells treated only with prazosin, intracellular prazosin accumulation decreased by 69% compared with that in MDCKII-mock cells ($p < 0.001$), indicating that BCRP actively transported prazosin out of the cells (Fig. 1B). However, co-treatment with the positive control inhibitor (novobiocin; 5 μM) restored prazosin accumulation to levels similar to those observed in MDCKII-mock cells, confirming the effective inhibition of BCRP.

Among the 77 flavonols tested, 22 compounds exhibited more than 25% inhibition of BCRP activity at a concentration of 2 μM (Fig. 1C and D). Notably, 3,4′-dimethoxyflavone (compound no. 37) demonstrated the strongest inhibitory effect, achieving 62% inhibition of BCRP at 2 μM. Additionally, several other compounds exhibited potent BCRP inhibition, including 3,5,7,3′,4′-pentahydroxyflavone (compound no. 27), 3,5,7,4′-tetrahydroxy-3′-methoxyflavone (compound no. 29), 4′-hydroxy-3,7,3′-trimethoxyflavone (compound no. 43), 3,6,3′,4′-tetramethoxyflavone (compound no. 46), and 3,5,6,7,3′,4′-hexamethoxyflavone (compound no. 54), with inhibition rates of 45.9%, 45.5%, 45.2%, 49.9%, and 52.0%, respectively, at a concentration of 2 μM. Overall, 22 flavonols were identified as BCRP inhibitors with more than 25% inhibition at 2 μM. In MDCKII-mock cells, flavonol treatment did not significantly affect prazosin accumulation, suggesting that these compounds did not interfere with passive or endogenous transport systems of prazosin.

Inhibitory potency of flavonols on BCRP activity

IC_{50} values for BCRP activity were determined for 22 flavonols that inhibited more than 25% of BCRP activity at 2 μM (Table 1). The accumulation of prazosin gradually increased with increasing concentration of novobiocin, a positive BCRP inhibitor, in MDCKII-BCRP cells (Fig. 2). The IC_{50} of novobiocin for BCRP activity was 1.43 μM, consistent with previously reported values[11,14]. Flavanol IC_{50} values ranged from 0.5 μM to 20 μM, with 3,4′-dimethoxyflavone exhibiting the strongest BCRP inhibition (IC_{50} 1.62 μM; Table 1). Additionally, 13 flavonols (3,7-dihydroxyflavone, 3,7,3′-trihydroxyflavone, 3,5,7,3′,4′-pentahydroxyflavone, 3,5,7,4′-tetrahydroxy-3′-methoxyflavone, 3,5,7,3′,4′-pentahydroxy-8-methylflavone, 3,3′,4′-trimethoxyflavone, 4′-hydroxy-3,7,3′-trimethoxyflavone, 3,6,3′,4′-tetramethoxyflavone, 5,7,3′-trihydroxy-3,4′-dimethoxyflavone, 5-hydroxy-3,7,3′,4′-tetramethoxyflavone, 6,3′-dihydroxy-3,5,7,4′-tetramethoxyflavone, 3,5,6,7,4′-pentamethoxyflavone, and 3,5,6,7,3′,4′-hexamethoxyflavone) exhibited potent inhibitory effects on BCRP, with IC_{50} values below 5 μM. Two flavonols (3,5,7,2′,4′-pentahydroxyflavone and 3,6,2′,3′-tetramethoxyflavone) exhibited relatively weak inhibitory potency on BCRP (IC_{50} > 10 μM), while the remaining seven flavonols exhibited moderate inhibitory effects on BCRP, with IC_{50} values between 5 and 10 μM.

Compound no.	Name	IC_{50} (μM)
-	Novobiocin	1.43
4	3,3'-Dihydroxyflavone	5.61
7	3,7-Dihydroxyflavone	3.14
8	3,7,3'-Trihydroxyflavone	2.78
17	3,6-Dihydroxyflavone	6.73
26	3,5,7-Trihydroxyflavone (galangin)	5.40
27	3,5,7,3',4'-Pentahydroxyflavone (quercetin)	2.63
29	3,5,7,4'-Tetrahydroxy-3'-methoxyflavone (isorhamnetin)	3.50
31	3,5,7,2',4'-Pentahydroxyflavone (morin)	24.9
32	3,5,7,3',4'-Pentahydroxy-8-methylflavone	2.91
37	3,4'-Dimethoxyflavone	1.62
39	3,3',4'-Trimethoxyflavone	3.79
43	4'-Hydroxy-3,7,3'-trimethoxyflavone	2.31
44	3,6-Dimethoxyflavone	8.20
45	3,6,3'-Trimethoxyflavone	8.98
46	3,6,3',4'-Tetramethoxyflavone	1.69
47	3,6,2',3'-Tetramethoxyflavone	15.5
48	5,7,3'-Trihydroxy-3,4'-dimethoxyflavone	3.54
50	5-Hydroxy-3,7,3',4'-tetramethoxyflavone (retusin)	2.23
51	3,5,7-Trimethoxyflavone	7.06
52	6,3'-Dihydroxy-3,5,7,4'-tetramethoxyflavone	3.62
53	3,5,6,7,4'-Pentamethoxyflavone	3.62
54	3,5,6,7,3',4'-Hexamethoxyflavone	2.81

Table 1. IC_{50} values of flavonols on BCRP activity.

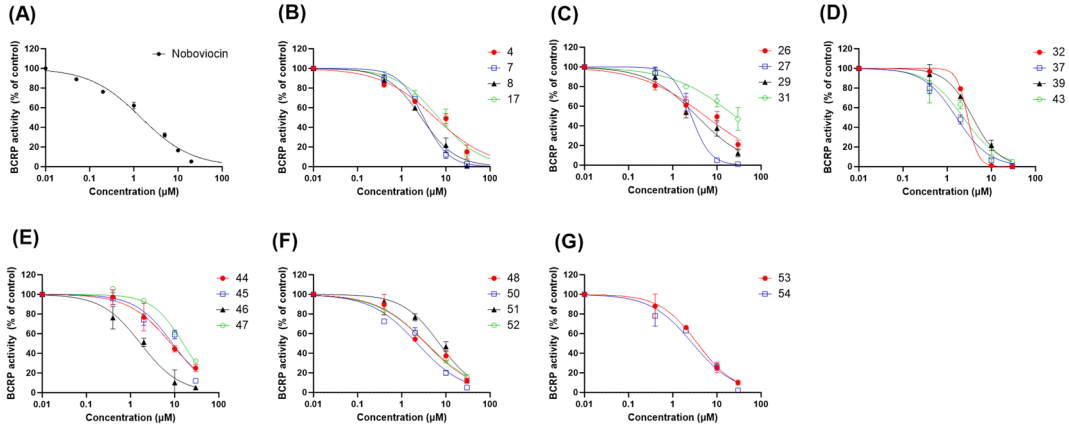

Fig. 2. Inhibitory potency of flavonols on BCRP activity in MDCKII-BCRP. Cells were treated with prazosin (5 μM) in the presence of various concentrations of novobiocin (0, 0.01, 0.5, 0.2, 1, 5, 10, and 20 μM;**A**) or 22 flavonols (0, 0.01, 0.4, 2, 10, and 30 μM; **B**–**G**) and then incubated for 20 min. Flavonols are presented with their compound number. Data are expressed as the mean ± SD of three independent biological replicates ($n = 3$).

Compound no.	Name	MDCKII-mock		MDCKII-BCRP		
		CC_{50} (μM)	RF_{mock}	CC_{50} (μM)	RF_{BCRP}	RF_t
-	Control	0.634	1.00	13.5	1.00	21.3
-	Novobiocin	0.821	1.29	2.47	0.183	3.01
7	3,7-Dihydroxyflavone	0.817	1.29	2.76	0.204	3.38
8	3,7,3'-Trihydroxyflavone	0.800	1.26	0.744	0.055	0.93
27	3,5,7,3',4'-Pentahydroxyflavone (quercetin)	0.676	1.07	0.921	0.068	1.36
29	3,5,7,4'-Tetrahydroxy-3'-methoxyflavone (isorhamnetin)	0.972	1.53	1.97	0.146	2.03
32	3,5,7,3',4'-Pentahydroxy-8-methylflavone	0.644	1.02	1.13	0.084	1.75
37	3,4'-Dimethoxyflavone	0.792	1.25	0.994	0.074	1.26
39	3,3',4'-Trimethoxyflavone	0.925	1.46	4.68	0.347	5.06
43	4'-Hydroxy-3,7,3'-trimethoxyflavone	0.804	1.27	0.955	0.071	1.19
46	3,6,3',4'-Tetramethoxyflavone	0.717	1.13	0.821	0.061	1.15
48	5,7,3'-Trihydroxy-3,4'-dimethoxyflavone	0.561	0.88	2.31	0.171	4.12
50	5-Hydroxy-3,7,3',4'-tetramethoxyflavone (retusin)	0.775	1.22	0.999	0.074	1.29
52	6,3'-Dihydroxy-3,5,7,4'-tetramethoxyflavone	0.801	1.26	3.58	0.265	4.47
53	3,5,6,7,4'-Pentamethoxyflavone	0.694	1.09	5.26	0.390	7.58
54	3,5,6,7,3',4'-Hexamethoxyflavone	0.810	1.28	1.91	0.141	2.36

Table 2. Effects of flavonols on BCRP-mediated resistance to SN-38. The reverse fold (RF) of flavonols was determined for each cell line (RF_{mock} and RF_{BCRP}) by comparing the CC_{50} values of SN-38 in the presence and absence of the inhibitors. The total reverse factor (RF_t) was calculated by dividing the CC_{50} of SN-38 in MDCKII-BCRP cells by the CC_{50} in MDCKII-mock cells.

Overcoming BCRP-mediated drug resistance by flavonols

To investigate the functional implications of flavonol-mediated BCRP inhibition, we assessed the cytotoxicity of SN-38, a BCRP substrate, in the presence of flavonols. BCRP reversed the cytotoxicity induced by SN-38 treatment by increasing the CC_{50} values of SN-38 from 0.634 to 13.5 μM. In contrast, novobiocin, a positive inhibitor of BCRP, decreased the CC_{50} values of SN-38 to 2.47 in MDCKII-BCRP cells, implying that BCRP inhibition recovered the cytotoxic effects of SN-38 (Table 2; Fig. 3).

Fourteen flavonols, the selected BCRP inhibitors, were added to the cells along with SN-38. In all the groups, treatment with flavonols did not significantly alter the viability of MDCKII-mock cells, indicating that the effect of the selected flavonols on cell viability was negligible in this experimental system. Among the 14 flavonols, six (3,7,3′-trihydroxyflavone, 3,5,7,3′,4′-pentahydroxyflavone, 3,4′-dimethoxyflavone, 4′-hydroxy-3,7,3′-trimethoxyflavone, 3,6,3′,4′-tetramethoxyflavone, and 5-hydroxy-3,7,3′,4′-tetramethoxyflavone) decreased the CC_{50} values in MDCKII-BCRP cells to levels comparable to those in mock cells, implying that these flavonols almost completely reversed BCRP-mediated resistance to SN-38. Additionally, 3,5,7,4′-tetrahydroxy-3′-

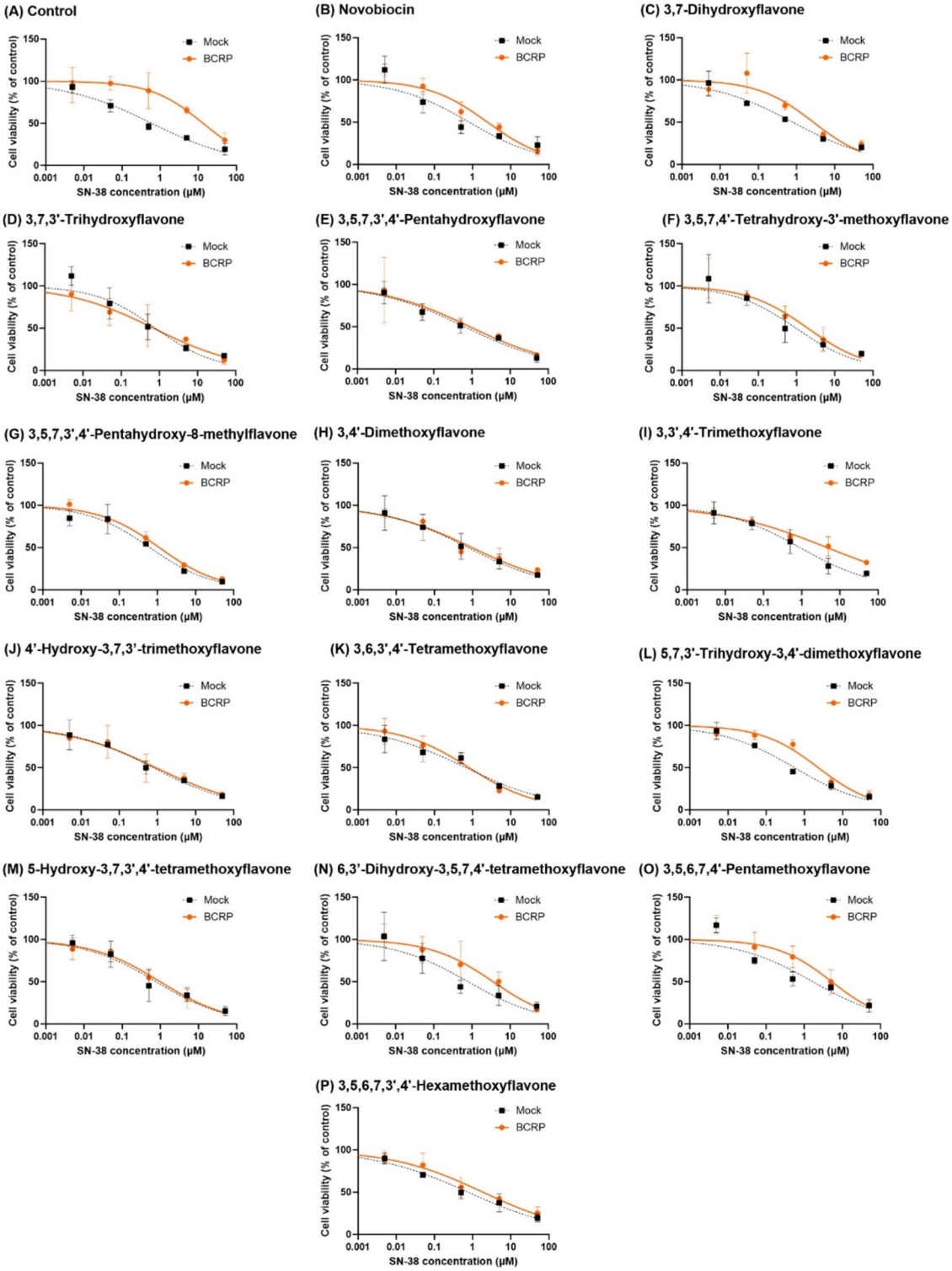

Fig. 3. Effects of flavonols on cell viability in SN-38-treated cells. Cell viability was determined by MTT assay without (**A**) or with novobiocin (5 μM; **B**) and flavonols (5 μM; **C**–**P**) in MDCKII-mock (dotted line with black squares) and MDCKII-BCRP cells (solid line with orange circles). Data are expressed as mean ± SD ($n = 3$).

methoxyflavone, 3,5,7,3′,4′-pentahydroxy-8-methylflavone, and 3,5,6,7,3′,4′-hexamethoxyflavone significantly altered CC_{50} values in MDCKII-BCRP cells, with RF_t values of 2.03, 1.75, and 2.36, respectively (Table 2).

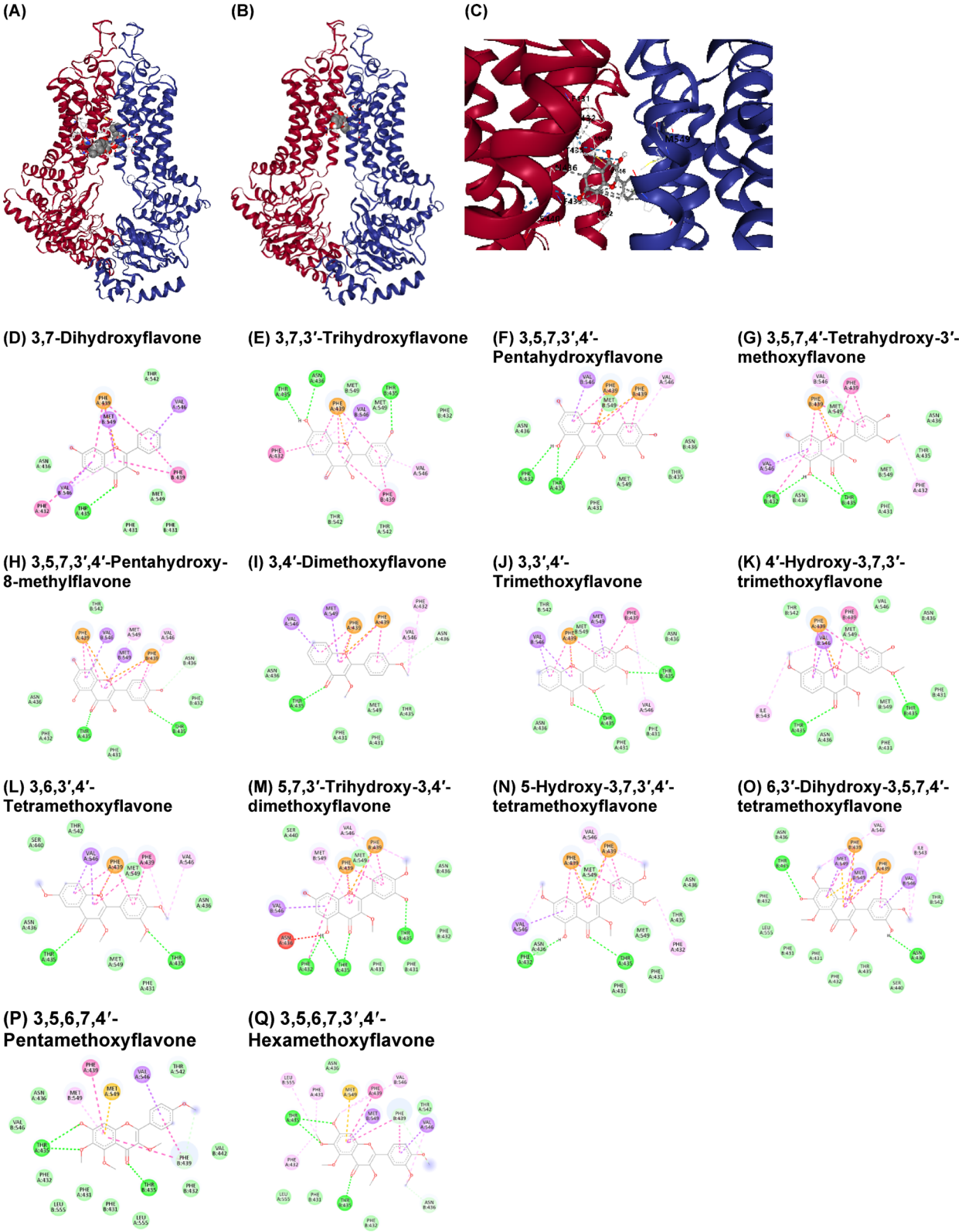

Molecular Docking results

A molecular docking study was conducted to predict the interactions between BCRP and flavonols, identified as potent BCRP inhibitors, using in silico analysis. To first evaluate the suitability of our docking model, we confirmed the binding interaction of novobiocin, a known BCRP inhibitor, which showed expected strong binding affinity (binding affinity: −10.8 kcal/mol; Fig. 4A). Among the 14 flavonols that strongly inhibited BCRP (IC_{50} < 5 μM) and reversed drug resistance against SN-38 in vitro, all exhibited binding affinities lower than − 8.5 kcal/mol, indicating very strong binding to BCRP (Table 3).

◀**Fig. 4**. Molecular docking of novobiocin and flavonols to BCRP. (**A**) Docking results between novobiocin, a representative BCRP inhibitor, and BCRP. (**B** and **C**) Representative docking results between 3,7-dihydroxyflavone (compound no. 7) and BCRP. Docking was conducted using CB-Dock 2 (https://cadd.labshare.cn/cb-dock2) and the interaction between the BCRP transporter and flavonols was analyzed using BIOVIA Discovery Studio Visualizer v24.1.0. (**D**–**Q**) The two-dimensional diagrams of potential amino acid residues of BCRP involved in binding with 14 flavonols. The residue colors indicate the types of interactions as follows: dark green (conventional hydrogen bonds), light green (Van der Waals interactions), deep pink (π-sigma interactions), pink (π- π stacking interactions), pale pink (alkyl interactions), orange (π-cation interactions), and red (unfavorable donor-donor interactions).

Compound no.	Compound	Binding affinity (kcal/mol)
-	Novobiocin	−10.8
7	3,7-Dihydroxyflavone	−9.1
8	3,7,3'-Trihydroxyflavone	−9.5
27	3,5,7,3',4'-Pentahydroxyflavone (quercetin)	−9.3
29	3,5,7,4'-Tetrahydroxy-3'-methoxyflavone (isorhamnetin)	−9.8
32	3,5,7,3',4'-Pentahydroxy-8-methylflavone	−10.4
37	3,4'-Dimethoxyflavone	−9.3
39	3,3',4'-Trimethoxyflavone	−9.7
43	4'-Hydroxy-3,7,3'-trimethoxyflavone	−9.0
46	3,6,3',4'-Tetramethoxyflavone	−9.3
48	5,7,3'-Trihydroxy-3,4'-dimethoxyflavone	−9.7
50	5-Hydroxy-3,7,3',4'-tetramethoxyflavone (retusin)	−9.7
52	6,3'-Dihydroxy-3,5,7,4'-tetramethoxyflavone	−9.2
53	3,5,6,7,4'-Pentamethoxyflavone	−8.7
54	3,5,6,7,3',4'-Hexamethoxyflavone	−9.2

Table 3. Predicted binding affinity between BCRP and flavonols.

Molecular docking analysis confirmed that all 14 flavonols analyzed were predicted to bind within the same region of the BCRP binding pocket (Fig. 4B and Q). PHE A:432 and PHE B:439 were critical for π-stacking interactions, whereas THR A:435 and ASN A:436 facilitated hydrogen bonding. Hydrophobic residues, including MET B:549 and VAL B:546, contributed to van der Waals and π-alkyl interactions, stabilizing the complexes. Structural modifications, such as hydroxylation and methylation, significantly influenced binding affinity. Highly hydroxylated compounds, including 3,5,7,3′,4′-pentahydroxyflavone (compound no. 27), formed strong hydrogen bonds, whereas methoxy-substituted compounds, such as 3,3′,4′-trimethoxyflavone (compound no. 39), favored hydrophobic interactions. Compounds with balanced functional groups, such as 3,5,6,7,3′,4′-hexamethoxyflavone (compound no. 54), exhibited diverse and strong binding profiles.

In vivo interactions with flavonols

We investigated the in vivo pharmacokinetic interactions of two flavonols—3,4′-dimethoxyflavone and 3,6,3′,4′-tetramethoxyflavone—that demonstrated potent BCRP inhibition in vitro. In this study, sulfasalazine, a well-established selective BCRP substrate, was administered orally, either alone or in combination with one of the flavonols, to rats. The plasma concentrations of both sulfasalazine and the flavonols were subsequently measured.

Following oral administration of sulfasalazine alone in rats, the drug was rapidly absorbed, reaching a C_{max} of 80.1 ± 15.2 ng/mL at 0.438 ± 0.125 h. The AUC_{last} and AUC_{inf} were 183 ± 84 and 223 ± 99 ng/mL·h, respectively, with an $t_{1/2}$ of 2.30 ± 1.76 h. Co-administration with 3,4′-dimethoxyflavone (5 mg/kg) markedly increased exposure to sulfasalazine. Specifically, the C_{max} increased by approximately 1.83-fold and AUC_{last} by 1.79-fold (327 ± 36 ng/mL·h), with the increase in AUC_{last} reaching statistical significance ($p < 0.05$). However, the $t_{1/2}$ (1.76 ± 0.29 h) was not significantly different from that observed when sulfasalazine was administered alone. When sulfasalazine was co-administered with 3,6,3′,4′-tetramethoxyflavone (5 mg/kg), C_{max} and AUC_{last} increased significantly, reaching 162 ± 19 ng/mL ($p < 0.001$) and 319 ± 25 ng/mL·h ($p < 0.05$), respectively, which were 2.02 and 1.74-fold higher than those in the control group. The $t_{1/2}$ in this group (2.34 ± 1.23 h) was similar to that observed with sulfasalazine alone (Table 4; Fig. 5A and B).

In the combination group (sulfasalazine + 3,4′-dimethoxyflavone or sulfasalazine + 3,6,3′,4′-tetramethoxyflavone), systemic exposure to 3,4′-dimethoxyflavone and 3,6,3′,4′-tetramethoxyflavone was low. Following an oral dose of 3,4′-dimethoxyflavone (5 mg/kg), a C_{max} of 13.5 ± 8.8 ng/mL was reached at 0.5 h, with an AUC_{last} of 12.4 ± 5.0 ng/mL·h and a short $t_{1/2}$ of 0.54 ± 0.15 h, rendering the compound undetectable after 2 h (Fig. 5C). Similarly, 3,6,3′,4′-tetramethoxyflavone reached a C_{max} of 13.3 ± 0.6 ng/mL, an AUC_{last} of 22.3 ± 1.6 ng/mL·h, and exhibited a $t_{1/2}$ of 2.24 ± 0.17 h (Fig. 5D).

Parameter	Sulfasalazine			3,4'-Dimethoxyflavone	3,6,3',4'-Tetramethoxyflavone
	Control	+ 3,4'-Dimethoxyflavone	+ 3,6,3',4'-Tetramethoxyflavone		
C_{max} (ng/mL)	80.1 ± 15.2	146.4 ± 58.4	162 ± 19 ***	13.5 ± 8.8	13.3 ± 0.6
T_{max} (h)	0.438 ± 0.125	0.5 ± 0	0.5 ± 0	0.5 ± 0	0.375 ± 0.144
$t_{1/2}$ (h)	2.3 ± 1.76	1.76 ± 0.29	2.34 ± 1.23	0.54 ± 0.15	2.24 ± 0.17
AUC_{last} (ng·h/mL)	183 ± 84	327 ± 36 *	319 ± 25 *	12.4 ± 5.0	22.3 ± 1.6
AUC_{inf} (ng·h/mL)	223 ± 99	356 ± 41 *	396 ± 88 *	13.3 ± 4.3	26.8 ± 2.5

Table 4. Pharmacokinetic parameters of sulfasalazine and flavonols following oral administration of sulfasalazine (2 mg/kg) with or without flavonols (5 mg/kg) in rats ($n = 5$, mean ± SD). AUC_{inf}, area under the plasma concentration–time curve from time 0 to infinity; AUC_{last}, area under the plasma concentration–time curve from time zero to the last quantifiable point; C_{max}, maximum concentration; T_{max}, time to reach C_{max}; $t_{1/2}$, half-life. * and *** denote $p < 0.05$ and $p < 0.001$, respectively, compared to the control group.

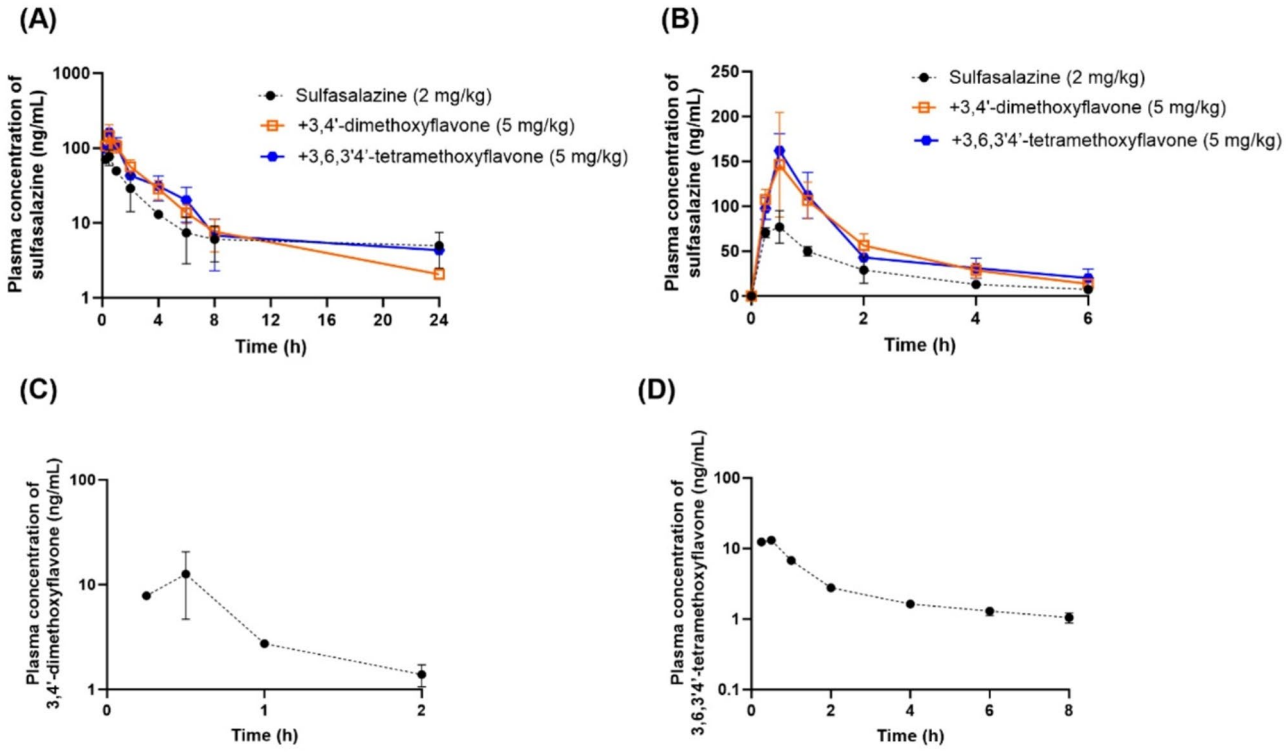

Fig. 5. Plasma concentration–time profile of sulfasalazine [**A** (0–24 h; semi-log scale) and **B** (0–6 h; linear scale)], 3,4′-dimethoxyflavone (**C**), and 3,6,3′,4′-tetramethoxyflavone (**D**). Rats were orally administered sulfasalazine (2 mg/kg) without or with 3,4′-dimethoxyflavone and 3,6,3′,4′-tetramethoxyflavone (5 mg/kg). Data are expressed as the mean ± SD ($n = 5$).

Discussion

This study investigated the interactions between flavonols and BCRP to assess the potential of flavonols as inhibitors to overcome BCRP-mediated drug resistance and modulate pharmacokinetics. Initially, 77 flavonols were screened, and 22 candidates with BCRP inhibitory activity were identified. Notably, 14 of these compounds exhibited IC_{50} values below 5 μM and effectively restored sensitivity to SN-38 in BCRP-overexpressing cells, indicating their ability to reverse drug resistance mediated by BCRP. To further investigate these findings in vivo, two representative flavonols—3,4′-dimethoxyflavone and 3,6,3′,4′-tetramethoxyflavone—were co-administered with sulfasalazine, a well-known BCRP substrate. Both compounds significantly increased systemic exposure to sulfasalazine, as evidenced by the elevated C_{max} and AUC values. These results suggest that flavonols can modulate BCRP activity in vivo, potentially enhancing the bioavailability of BCRP substrate drugs and mitigating drug resistance.

Several studies have demonstrated that flavonoids act as potent inhibitors of BCRP. For example, Fan et al. reported that amentoflavone, a biflavone, effectively inhibits BCRP with an IC_{50} of approximately 4 μM[23]. This study also showed that co-administration of amentoflavone (30 mg/kg) with mitoxantrone increased the AUC of mitoxantrone by 1.23-fold in rats, indicating in vivo relevance of BCRP inhibition. In addition to amentoflavone,

well-characterized flavonoids such as quercetin and retusin have been widely recognized in the literature as effective BCRP inhibitors[23,28]. These compounds have been reported to inhibit BCRP-mediated drug efflux, thereby enhancing intracellular accumulation of chemotherapeutic agents and reversing multidrug resistance. Our current findings are consistent with these established reports, as we observed comparable or improved IC_{50} values for these flavonols, further confirming their potent inhibitory effects. The work by Pick et al. provided detailed insights into the structure–activity relationships (SAR) of flavonoids as BCRP inhibitors using both 2D and 3D QSAR approaches[29]. Their findings highlight key structural features that significantly impact inhibitory potency. Our current findings align well with these SAR patterns, and we observed comparable or improved IC_{50} values for flavonols containing similar functional groups. Moreover, our study advances the field by focusing specifically on the flavonol subclass and systematically analyzing structure-activity relationships through molecular docking combined with functional assays. This targeted approach complements prior broader flavonoid studies and provides more precise insights into the chemical features critical for BCRP inhibition. Taken together, these data corroborate the well-documented inhibitory activity of flavonoids like quercetin and retusin against BCRP and support their continued exploration as promising scaffolds for the development of novel BCRP inhibitors.

Both BCRP and MDR1 are frequently overexpressed in various cancer types, contributing to multidrug resistance. However, the expression profiles of these transporters can vary significantly between tumor types and even among patients within the same cancer subtype. In some cases, tumors may predominantly express one transporter over the other. Notably, many flavonoids have been reported to inhibit MDR1 as well as BCRP, demonstrating a broad-spectrum inhibitory activity against multiple efflux transporters[22]. Given this variability and the multi-transporter inhibitory potential of flavonoids, it is important to consider their specificity toward BCRP and MDR1 in the context of the target cancer type. Tailoring the selection and application of flavonoid inhibitors based on the transporter expression pattern of the tumor could enhance therapeutic efficacy and reduce off-target effects. This approach underscores the need for detailed characterization of flavonoid transporter selectivity to inform precision medicine strategies in overcoming drug resistance.

Molecular docking analysis identified key amino acid residues and interaction types involved in the binding between flavonols and BCRP, providing insights into the structural determinants of binding affinity. Among the most frequently interacting residues, PHE A:439 and PHE B:439 played a pivotal role in π-stacking interactions, stabilizing the aromatic rings of the flavonoids, while THR A:435 and ASN A:436 were critical for forming hydrogen bonds, adding specificity and stability to the flavonoid-BCRP complexes. Hydrophobic residues, such as MET B:549 and VAL B:546, contributed to van der Waals and π-alkyl interactions, further stabilizing the flavonoid binding. The analysis revealed that structural features, such as hydroxylation and methylation, significantly influenced the binding affinity and interaction profiles. Hydroxyl groups enhanced polar interactions, forming strong hydrogen bonds with residues like THR A:435, as observed in the highly hydroxylated flavonoids such as 3,5,7,3′,4′-pentahydroxyflavone. In contrast, methoxy groups promoted hydrophobic and π-alkyl interactions, as seen in compounds like 3,3′,4′-trimethoxyflavone, which interacted extensively with PHE A:439 and VAL B:546. Compounds with balanced substitutions, such as 3,5,6,7,3′,4′-hexamethoxyflavone, exhibited diverse interaction profiles, engaging in hydrogen bonding, van der Waals forces, and π-stacking interactions, making them particularly effective in binding BCRP. These findings underscore the importance of residue-specific interactions and the impact of structural modifications on binding affinity, providing a framework for designing flavonoid-based BCRP inhibitors to enhance therapeutic efficacy and overcome multidrug resistance.

Despite these promising results, several limitations of this study must be acknowledged. Although the in vivo studies confirmed that 3,4′-dimethoxyflavone and 3,6,3′,4′-tetramethoxyflavone enhanced exposure to a BCRP substrate, their own systemic concentrations were very low, suggesting that their primary site of action may be within the intestinal lumen rather than systemic circulation. This raises the possibility that, while these compounds might be useful for improving the bioavailability of BCRP substrate drugs or overcoming drug resistance in gastrointestinal tract cancers, such as colorectal cancer, they may be less effective in reversing BCRP-mediated drug resistance in tumors located in other tissues. Nonetheless, the structure–activity insights from our study provide a basis for the synthesis of derivatives with improved oral bioavailability, which could potentially achieve therapeutic concentrations in the systemic circulation and target tissues.

Another limitation is the interspecies differences between in vitro and in vivo models. While in *vitro* studies have used human BCRP, in vivo experiments have only been conducted in rats. Despite an 81.2% amino acid sequence homology between human and rodent BCRP , significant differences may remain in other regions, potentially limiting interspecies extrapolation. Additionally, tissue-specific BCRP expression levels differ between species. Although similar expression patterns have been observed in the liver and brain microvessels of humans and rats, the kidneys exhibit higher BCRP expression in rats than in humans, which may influence drug pharmacokinetics[23,28]. Moreover, direct comparisons of intestinal BCRP expression between humans and rats are limited. These differences and the limited information underscore the need for caution when extrapolating rat data to humans, highlighting the importance of conducting clinical drug interaction studies to validate these findings. Future research should aim to bridge these gaps through clinical trials and detailed comparative studies of BCRP expression and function in human and animal models. In addition to addressing interspecies differences, it should be noted as a limitation of our study that SN-38, the active metabolite of irinotecan and a well-established BCRP substrate, was not utilized as the probe substrate in our in vivo experiments. Consequently, the reversal of SN-38 resistance by BCRP inhibition was only demonstrated in vitro, whereas the in vivo pharmacokinetic interaction study used sulfasalazine as the model BCRP substrate. Given that different BCRP substrates can yield varying outcomes in transporter-mediated drug interactions, future studies are needed to evaluate the effect of these flavonols on the pharmacokinetics of SN-38 in vivo. Future work should also evaluate the potential chemotherapeutic benefit of these flavonols in tumor-bearing models and systematically investigate their toxicity and possible off-target effects in non-tumor tissues, as flavonoids

can interact with other transporters and metabolic pathways. Such studies will be critical for advancing these findings toward clinical application.

Multiple experimental approaches are available for assessing BCRP inhibitory activity, each providing distinct and complementary insights into transporter function. In the present study, we utilized accumulation study to evaluate the inhibitory effects of flavonols on BCRP-mediated efflux. While accumulation study effectively quantifies inhibition of substrate transport, other methodologies such as transport assays, ATPase activity measurements, and flow cytometry-based analyses are also widely employed in the field. Flow cytometry, in particular, offers the advantage of directly measuring intracellular substrate accumulation at the single-cell level, allowing for detailed analysis of cell population heterogeneity. It is also important to consider that some compounds, including quercetin, may act as both inhibitors and substrates of BCRP . Therefore, a comprehensive evaluation of inhibitory profiles requires integration of multiple complementary methods to account for such dual roles and to better elucidate the mechanisms of interaction with the transporter.

Conclusions

In conclusion, this study identified flavonols with potent BCRP inhibitory effects and provided mechanistic insights into their interactions with this transporter. These findings advance our understanding of flavonol-BCRP interactions and their potential applications in addressing multidrug resistance and optimizing drug therapies. Future research should focus on enhancing the systemic exposure to these flavonols and validating their efficacy in clinical settings to fully harness their therapeutic potential.

Data availability

The datasets used and analyzed during the current study are available from the corresponding author on reasonable request.

Received: 30 May 2025; Accepted: 28 July 2025
Published online: 05 August 2025

References

1. Jani, M. et al. Structure and function of BCRP, a broad specificity transporter of xenobiotics and endobiotics. *Arch. Toxicol.* **88**, 1205–1248 (2014).
2. Beéry, E. et al. ABCG2 modulates Chlorothiazide permeability in vitro–characterization of its interactions. *Drug Metab. Pharmacokinet.* **27**, 349–353 (2012).
3. Jani, M. et al. Kinetic characterization of sulfasalazine transport by human ATP-binding cassette G2. *Biol. Pharm. Bull.* **32**, 497–499 (2009).
4. Choi, M. K., Lee, J. & Song, I. S. Pharmacokinetic modulation of substrate drugs via the Inhibition of drug-metabolizing enzymes and transporters using pharmaceutical excipients. *J. Pharm. Invest.* **53**, 1–18 (2023).
5. Gulnaz, A. et al. A mechanism-based Understanding of altered drug pharmacokinetics by gut microbiota. *J. Pharm. Invest.* **53**, 73–92 (2023).
6. Chae, Y. J. et al. Regulation of drug transporters by MicroRNA and implications in disease treatment. *Journal Pharm. Investigation* **52**, 23–47 (2022).
7. Maliepaard, M. et al. Subcellular localization and distribution of the breast cancer resistance protein transporter in normal human tissues. *Cancer Res.* **61**, 3458–3464 (2001).
8. Jigorel, E., Le Vee, M., Boursier-Neyret, C., Parmentier, Y. & Fardel, O. Differential regulation of sinusoidal and canalicular hepatic drug transporter expression by xenobiotics activating drug-sensing receptors in primary human hepatocytes. *Drug Metab. Dispos.* **34**, 1756–1763 (2006).
9. van de Wetering, K. et al. Intestinal breast cancer resistance protein (BCRP)/Bcrp1 and multidrug resistance protein 3 (MRP3)/Mrp3 are involved in the pharmacokinetics of Resveratrol. *Mol. Pharmacol.* **75**, 876–885 (2009).
10. Lee, J., Kim, J., Kang, J. & Lee, H. J. COVID-19 drugs: potential interaction with ATP-binding cassette transporters P-glycoprotein and breast cancer resistance protein. *J. Pharm. Invest.* **53**, 191–212 (2023).
11. Elsby, R. et al. Mechanistic in vitro studies indicate that the clinical drug-drug interactions between protease inhibitors and Rosuvastatin are driven by Inhibition of intestinal BCRP and hepatic OATP1B1 with minimal contribution from OATP1B3, NTCP and OAT3. *Pharmacol. Res. Perspect.* **11**, e01060 (2023).
12. Zhang, W. et al. Role of BCRP 421C > A polymorphism on Rosuvastatin pharmacokinetics in healthy Chinese males. *Clin. Chim. Acta*. **373**, 99–103 (2006).
13. Vora, B. et al. Oxypurinol pharmacokinetics and pharmacodynamics in healthy volunteers: influence of BCRP Q141K polymorphism and patient characteristics. *Clin. Transl. Sci.* **14**, 1431–1443 (2021).
14. Elsby, R., Martin, P., Surry, D., Sharma, P. & Fenner, K. Solitary Inhibition of the breast cancer resistance protein efflux transporter results in a clinically significant Drug-Drug interaction with Rosuvastatin by causing up to a 2-Fold increase in Statin exposure. *Drug Metab. Dispos.* **44**, 398–408 (2016).
15. Robey, R. W., Polgar, O., Deeken, J., To, K. W. & Bates, S. E. ABCG2: determining its relevance in clinical drug resistance. *Cancer Metastasis Rev.* **26**, 39–57 (2007).
16. Hu, L. L. et al. BCRP gene polymorphisms are associated with susceptibility and survival of diffuse large B-cell lymphoma. *Carcinogenesis* **28**, 1740–1744 (2007).
17. Chen, P. et al. The contribution of the ABCG2 C421A polymorphism to cancer susceptibility: a meta-analysis of the current literature. *BMC Cancer*. **12**, 383 (2012).
18. Panche, A. N., Diwan, A. D. & Chandra, S. R. Flavonoids: an overview. *J. Nutritional Sci.* **5**, e47 (2016).
19. Darband, S. G. et al. Quercetin: a functional dietary flavonoid with potential chemo-preventive properties in colorectal cancer. *J. Cell. Physiol.* **233**, 6544–6560 (2018).
20. Verma, V. K. et al. Role of MAPK/NF-κB pathway in cardioprotective effect of Morin in isoproterenol induced myocardial injury in rats. *Mol. Biol. Rep.* **46**, 1139–1148 (2019).
21. Shin, K. H., Lee, K. R., Kang, M. J. & Chae, Y. J. Strong Inhibition of organic cation transporter 2 by flavonoids and Attenuation effects on cisplatin-induced cytotoxicity. *Chemico-Biol. Interact.* **379**, 110504 (2023).
22. Kang, M. J., Lee, K. R., Choi, Y. J. & Chae, Y. J. Identification of flavonol derivatives inhibiting MDR1: a strategy to overcome multidrug resistance in cancer. *Natural Prod. Research.* **5**, 1–9 (2024).
23. Fan, X. et al. Evaluation of inhibitory effects of flavonoids on breast cancer resistance protein (BCRP): from library screening to biological evaluation to structure-activity relationship. *Toxicol. Vitro: Int. J. Published Association BIBRA*. **61**, 104642 (2019).

24. Song, Y. K. et al. Suppression of canine ATP binding cassette ABCB1 in Madin-Darby canine kidney type II cells unmasks human ABCG2-Mediated efflux of Olaparib. *J. Pharmacol. Exp. Ther.* **368**, 79–87 (2019).
25. Song, Y. K. et al. Role of the efflux transporters Abcb1 and Abcg2 in the brain distribution of Olaparib in mice. *Eur. J. Pharm. Sci.* **173**, 106177 (2022).
26. Kang, M. J. et al. Interactions of bosutinib with drug transporters: in vitro and in vivo Inhibition of organic cation transporter 2, multidrug and toxin extrusion protein 1, and breast cancer resistance protein by bosutinib. *Biomed. Pharmacother.* **178**, 117114 (2024).
27. Liu, Y. et al. CB-Dock: A web server for cavity detection-guided protein–ligand blind Docking. *Acta Pharmacol. Sin.* **41**, 138–144 (2020).
28. Fallon, J. K., Smith, P. C., Xia, C. Q. & Kim, M. S. Quantification of four efflux drug transporters in liver and kidney across species using targeted quantitative proteomics by isotope Dilution NanoLC-MS/MS. *Pharm. Res.* **33**, 2280–2288 (2016).
29. Pick, A. et al. Structure–activity relationships of flavonoids as inhibitors of breast cancer resistance protein (BCRP). *Bioorg. Med. Chem.* **19**, 2090–2102 (2011).

Acknowledgements

The chemical library used in this study was provided by the Korea Chemical Bank (www.chembank.org) of Korea Research Institute of Chemical Technology.

Author contributions

K.-R. Lee: Conceptualization, data curation, formal analysis, software, writing the original draft, and funding acquisition. M.-J. Kang: Conceptualization, data curation, methodology, investigation, and writing – original draft. M.-J. Kim: Methodology, investigation, and writing – original draft. Y. Im: Data curation, methodology, investigation, and writing – original draft. H.-C. Jeong: Methodology, investigation, and writing – original draft. Y.-J. Chae: Conceptualization, investigation, methodology, writing – review and editing, supervision, project administration, and funding acquisition.

Funding

This research was supported by the Basic Science Research Program through the National Research Foundation (NRF) of Korea, funded by the Ministry of Education (2021R1I1A3056261), a grant from the KRIBB Research Initiative Program, and a grant from the Korea Machine Learning Ledger Orchestration for Drug Discovery Project (K-MELLODDY), funded by the Ministry of Health & Welfare and the Ministry of Science and ICT, Republic of Korea (RS-2024-00459727).

Declarations

Competing interests

The authors declare no competing interests.

Arrive statement

All animal procedures were performed in accordance with ARRIVE guidelines.

Additional information

Supplementary Information The online version contains supplementary material available at https://doi.org/10.1038/s41598-025-13908-1.

Correspondence and requests for materials should be addressed to Y.-J.C.